IOP Conf. Series: Materials Science and Engineering **396** (2018) 012035 doi:10.1088/1757-899X/396/1/012035

Synthesis, structure and characterization of Co doped CeO_2 nanoparticles

Saurabh Tiwari[a], Nivedha Balasubramanian[b], Sajal Biring[c], Somaditya Sen[a,*]

[a]Metallurgical Engineering and Material Sciences, Indian Institute of Technology Indore, India

[b]Department of Physics, PSG College of Arts and Science, Coimbatore, India

[c]Electronic Engg., Ming Chi University of Technology, New Taipei City, Taiwan

E-mail: sens@iiti.ac.in

Abstract. Nanocrystalline Co doped CeO_2 particles were synthesized using simple sol-gel method. The structural, vibrational and photoluminescence properties of synthesized nanoparticles were investigated using X-ray power diffraction (XRD), UV-visible spectroscopy, Raman spectroscopy and Photolumiscence (PL) spectroscopy. XRD showed that the lattice shrink and crystallite size decreases with doping which leads to lattice distortion and generation of strain. The bandgap is red shifted due to formation of defects states between bandgap as confirmed by urbach energy calculation. The PL intensity of Co doped CeO_2 reduces which is due to the non radiative emission centres. Raman analysis showed characteristic peak at 460.8 cm^{-1} of Ce-O vibrational unit. A weak peak emerges with doping at ~ 540-640 cm^{-1} hints generation of oxygen vacancies related defects which also acts as emission quenching center.

1. Introduction

Cerium is one of the most abundant rare earth elements (66.5 ppm in earth crust) and its oxide (CeO_2) has high dielectric constant and bandgap. Nanocrystalline CeO_2 generally shows different physical and chemical properties than its bulk form and has superior physical and chemical properties which make it useful for various applications. It is used as electrolyte in solid oxide fuel cells (SOFC), as catalysis to controlling emission from vehicles, solar cells, as gas sensor, as phosphors, as polishing material etc. [1–6]. For tailoring the properties of material doping is one of the efficient tools. It is well observed that transition element doping in CeO_2 enhance its properties and increase its functionality. Among transition element doping Co doping has attracted much interest. As Ranjith *et al* reported enhancement in ferromagnetism at room temperature with Co doping in CeO_2 [7], Saranya *et al* reported increase in photocatalytic behavior of CeO_2 with Co doping using UV and visible light [8], Abbas *et al* found differential cytotoxicity of Co doped CeO_2 nanoparticles i.e does not affect healthy cell but inhibit the viability of Neuroblastoma cancer cell [9].

Different methods are used for preparing CeO_2 nanoparticles as wet chemical method, solution evaporation and decomposition method, solgel method, etc. We have used simple solgel method for synthesis of all samples since it is cost effective, low temperature and effective method for getting better homogeneity. The synthesized $Ce_{1-x}Co_xO_2$ nanoparticles were characterized for structural, vibrational and photoluminescence properties using XRD, UV-visible absorption, Raman and Photoluminescence spectroscopy. XRD shows generation of strain with doping which may be due to generation of defects and lattice distortion. Co doping affects bandgap and PL emission, the effect of oxygen vacancies discussed.

2. Experimental

Solgel method was used for synthesizing $Ce_{1-x}Co_xO_2$ samples. Cerium nitrate ($Ce(NO_3)_3.6H_2O$) and Cobalt nitrate ($Co(NO_3)_2.6H_2O$) of analytical grade were obtained from Alfa Aesar. These precursors were dissolved in double distilled de-ionized water and stirred in magnetic stirrer for 1 h. After that these two solutions were mixed and stirred for 2 h for homogeneous mixing. A solution of citric acid and glycerol was used for forming chelating chain and burning of the gel. This solution was mixed with the precursor's solution. The resulted solution was stirred and heated for 2 h at 80^0C which finally gives a black powder which was calcined at 450^oC for 6 h to get rid of carbon and nitrogen compounds. $Ce_{1-x}Co_xO_2$ samples were obtained for x=0 and x=0.05, which were further characterized.

X-ray Diffractometer (Bruker D2 Phaser) was used for investigating structural properties. UV-vis spectrophotometer (Shimadzu (UV-2600)) used for analyzing optical bandgap energy. Photoluminescence study was done using Perkin Elmer fluorescence spectrometer LS55, excitation wavelength 340nm. Vibrational properties were assessed using High Resolution Raman Micro Spectrometer, (HORIBA Scientific, 632.8nm).

3. Result and discussion

Fig. 1(a) shows the XRD spectra for synthesized $Ce_{1-x}Co_xO_2$ samples. All Peaks matches with prescribed CIF file-4343161 (Crystallography open database) confirming single phase cubic fluorite structure formation of CeO_2. No peaks correspond to oxide of Co or other impurities are present.

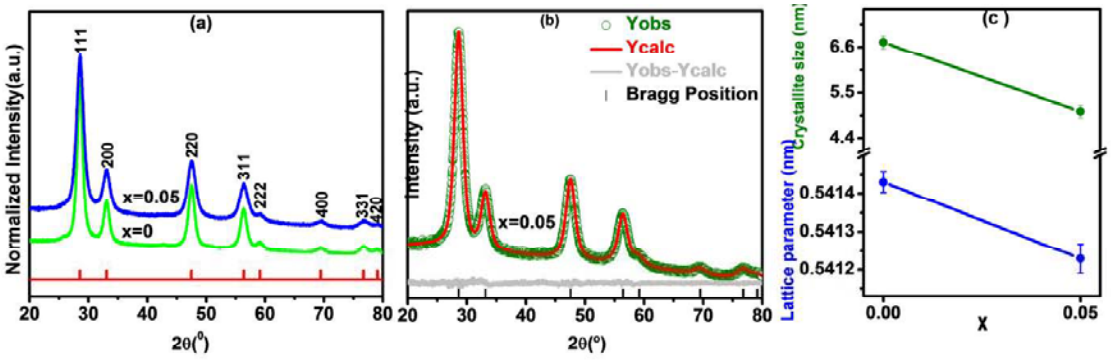

Fig.1. (a) XRD spectra of undoped and Co doped nanoparticles; (b) Rietvild refinement of Co doped CeO_2; (c) Lattice parameter and crystallite size variation with doping.

To observe the effect of Co doping in CeO_2, Reitveld refinement [fig. 1 (b)] was done using Fullprof suite software. Co doping cause lattice shrinkage as lattice parameter decreases with doping [fig. 1 (c)] this may be due to smaller ionic radii of $Co^{2+/3+}$ (0.75-0.9Å) than that of Ce^{4+} (0.97Å).

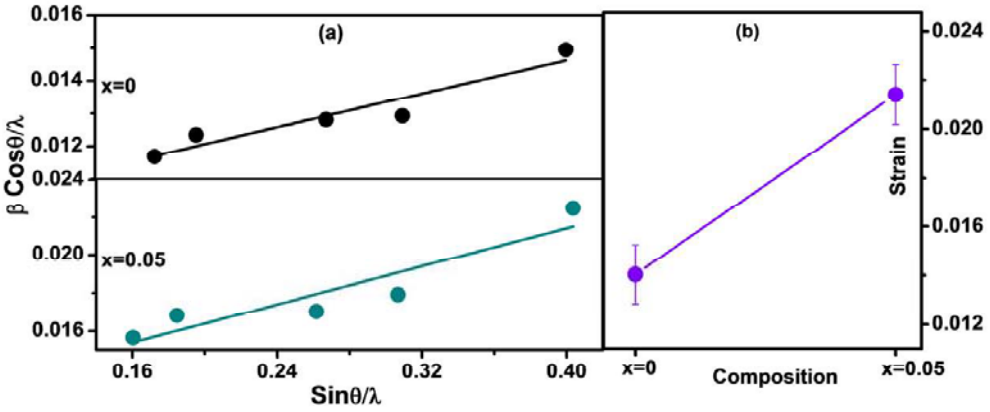

Fig. 2. (a) Williamson-Hall plot; (b) Strain variation with doping

This shrinkage should lead to lattice distortion and strain. Strain is calculated using Williamson-Hall (W-H) equation [10]; $\beta Cos\theta/\lambda = 1/D + \eta Sin\theta/\lambda$, where β is the full width half maxima (FWHM), θ is the angle of diffraction, λ is the wavelength of X-rays and D is crystallite size. A plot between $\beta Cos\theta/\lambda$ and $Sin\theta/\lambda$ plotted, slope η gives strain [Fig. 2 (a)]. It is found that strain is increasing with doping as expected [Fig. 2 (b)]. Crystallite size is calculated using formulae; $D = k\lambda/\beta cos\theta$ (k=0.9), found decreasing with doping this may be due to strain which restrict crystallite growth.

Optical properties of CeO_2 are of great interest in tuning its catalytic, biomedical and other activities. UV-visible spectroscopy depicts the absorption spectra of $Ce_{1-x}Co_xO_2$ (x=0 and x=0.05) nanoparticles samples [Fig. 3 (a)]. Kubelka-Munk function [11], $F(R) = (1-R)^2/2R$ used for calculating the bandgap as previously reported [12]. Co doping cause reduction of bandgap from 3.05 (x=0) to 2.52 eV (x=0.05) [Fig. 3 (b)]. This lowering of bandgap may be due to formation of some impurities band due to defects between valance band (VB) and conduction band (CB) [13]. Urbach energy (E_U): $\alpha = \alpha_0 * exp(E/Eu)$ accounts for defects in lattice, where α is coefficient of absorption, E is energy in eV.

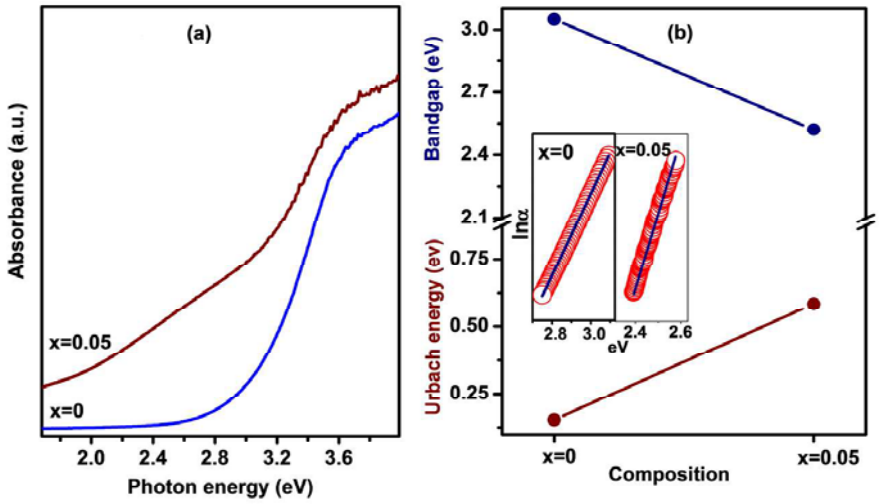

Fig. 3. (a) UV-visible absoption spectra; (b) Change in bandgap and urbach energy with doping (-inset shows urbach fitting)

The inverse of the slope of the plot between lnα and E give urbach energy. Urbach energy is increases with doping which confirm that defect states are increasing with doping [Fig. 3 (b)]. The effective gap between VB and CB reduces due to the deformation of electronic state.

Raman spectroscopy is very effective tool for obtaining structural information of fluorite structure because it is very sensitive to oxygen lattice vibration. [Figure 4 (a)] shows the Raman spectra of undoped and Co doped samples. A peak at 460.8 cm^{-1} is a characteristic F_{2g} symmetrical stretching mode of Ce-O vibrational unit [14]. This peak becomes broader and shift to lower wave number this may be due to generation of strain and reducing of Ce-O vibrational unit [Fig. 4 (b)]. A weak broad peak ~ 540-640 is due to generation of oxygen vacancies related defects Figure 4 (a)] [15]. Raman analysis supports urbach energy calculation regarding generation of defects which increases with doping.

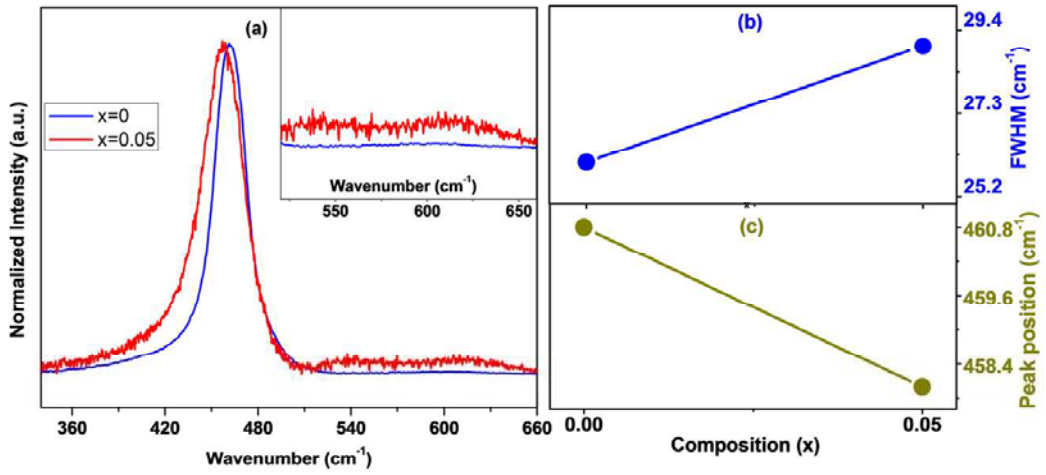

Fig. 4. (a) Raman spectra of $Ce_{1-x}Co_xO_2$ samples; (b, c) Variation in FWHM and peak position with doping.

The photoluminescence (PL) is an effective tool for analyzing defects and recombination process. Fig.5 shows the PL spectra of CeO_2, the peaks lying in between 395 and 529 are due to oxygen vacancies, surface defects and switching of charge between conduction band Ce^{4+} (4f) and valance band O^{2-} (2p) [16]. The emission bands are at ~424 nm correspond to surface defects, the band at ~457 nm and a feeble band at ~485 nm are considered as transition from ionized oxygen vacancies to the valance band and a band at ~528 nm reported as band due to defects as oxygen vacancies [17]. The PL emission intensity decreasing with doping, this infers the formation of defects states between valance and conduction band as confirmed by Raman and urbach calculation. The defects presents on surface and in bulk have different emissions one has non-radiative and other is having radiative emissions which affect the PL emission which depend on the nature of the oxygen vacancies. With Co doping in CeO_2, on the surface and on grain boundaries there is increase in oxygen vacancies which acts as trap centers leads to non-radiative recombination center and repress the emission intensity. Co doping causes high oxygen vacancies in CeO_2 matrix due to which spatial overlapping of electron and hole wave function obstructed which in turn prolong the recombination of charge carriers. Hence with Co doping surface defects increasing which cause non radiative emission and reduces the PL emission.

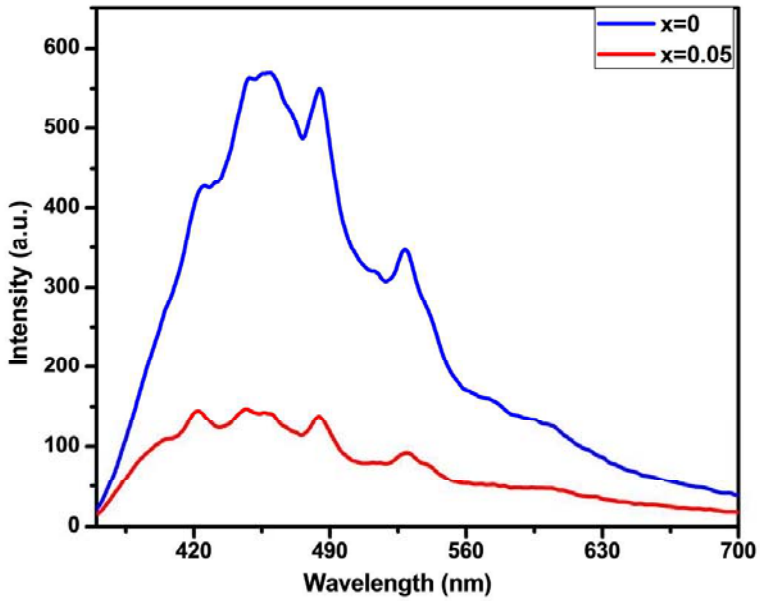

Fig. 5. Photoluminscence (PL) spectra of Ce1-xCoxO2 samples.

4. Conclusion

$Ce_{1-x}Co_xO_2$ (x=0 and x=0.05) nanoparticles have been successfully synthesized by simple sol-gel method. XRD and Raman analysis confirms the formation of cubic fluorite structure of undoped and Co doped CeO_2. Lattice shrinks and strain increases with doping. The estimated bandgap of undoped CeO_2 is 3.05 eV which decreases to 2.52 eV with Co doping. Urbach energy shows defects states are increasing which causes reduction of bandgap. A weak and broad peak ~540-640 pointing out that oxygen vacancies related defects are increasing with doping. The PL spectrum of CeO_2 has emission band from ~395-529 nm. The PL emission decreases with Co doping due to formation of oxygen vacancies related defects which act as non radiative emission center.

Acknowledgements

The authors would like to thank IIT Indore for the funding, Dr. Vipul Kumar Singh (IIT Indore) for Photoluminescence spectroscopy, Dr. V. K. Jain (Amity University, Noida, India) for UV-Vis measurement facility, Dr. Manoj kumar (IISER, Bhopal, India) for Raman spectroscopy.

Reference

[1] Murray E P, Tsai T and Barnett S A 1999 A direct-methane fuel cell with a ceria-based anode *Nature* **400** 649–51

[2] Fu Q, Saltsburg H and Flytzani-Stephanopoulos M 2003 Active Nonmetallic Au and Pt Species on Ceria-Based Water-Gas Shift Catalysts *Science* **301** 935–8

[3] Corma A, Atienzar P, García H and Chane-Ching J-Y 2004 Hierarchically mesostructured doped CeO2 with potential for solar-cell use *Nat. Mater.* **3** 394–7

[4] Izu N, Shin W, Murayama N and Kanzaki S 2002 Resistive oxygen gas sensors based on CeO2 fine powder prepared using mist pyrolysis *Sens. Actuators B Chem.* **87** 95–8

[5] Morshed A H, Moussa M E, Bedair S M, Leonard R, Liu S X and El-Masry N 1997 Violet/blue emission from epitaxial cerium oxide films on silicon substrates *Appl. Phys. Lett.* **70** 1647–9

[6] Lee S-H, Lu Z, Babu S V and Matijević E 2002 Chemical mechanical polishing of thermal oxide films using silica particles coated with ceria *J. Mater. Res.* **17** 2744–9

[7] Ranjith K S, Saravanan P, Chen S-H, Dong C-L, Chen C L, Chen S-Y, Asokan K and Rajendra Kumar R T 2014 Enhanced Room-Temperature Ferromagnetism on Co-Doped CeO2 Nanoparticles: Mechanism and Electronic and Optical Properties *J. Phys. Chem. C* **118** 27039–47

[8] Saranya J, Ranjith K S, Saravanan P, Mangalaraj D and Rajendra Kumar R T 2014 Cobalt-doped cerium oxide nanoparticles: Enhanced photocatalytic activity under UV and visible light irradiation *Mater. Sci. Semicond. Process.* **26** 218–24

[9] Abbas F, Iqbal J, Jan T, Naqvi M S H, Gul A, Abbasi R, Mahmood A, Ahmad I and Ismail M 2015 Differential cytotoxicity of ferromagnetic Co doped CeO2 nanoparticles against human neuroblastoma cancer cells *J. Alloys Compd.* **648** 1060–6

[10] Kuriakose S, Satpati B and Mohapatra S 2014 Enhanced photocatalytic activity of Co doped ZnO nanodisks and nanorods prepared by a facile wet chemical method *Phys. Chem. Chem. Phys.* **16** 12741–9

[11] Singh P, Choudhuri I, Rai H M, Mishra V, Kumar R, Pathak B, Sagdeo A and Sagdeo P R 2016 Fe doped LaGaO3: good white light emitters *RSC Adv.* **6** 100230–8

[12] Tiwari S, Bajpai G, Srivastava T, Viswakarma S, Shirage P, Sen S and Biring S 2017 Effect of strain due to Ni substitution in CeO2 nanoparticles on optical and mechanical properties *Scr. Mater.* **129** 84–7

[13] Veis M, Kucera M, Zahradnik M, Antos R, Mistrik J, Bi L, Kim H-S, Dionne G F and Ross C A 20140507 Optical and magneto-optical properties of Co-doped CeO2−δ films in the 0.5 to 4 eV range *J. Appl. Phys.*

[14] Weber W H, Hass K C and McBride J R 1993 Raman study of ${\mathrm{CeO}}_{2}$: Second-order scattering, lattice dynamics, and particle-size effects *Phys. Rev. B* **48** 178–85

[15] Bernardi M I B, Mesquita A, Béron F, Pirota K R, Zevallos A O de, Doriguetto A C and Carvalho H B de 2015 The role of oxygen vacancies and their location in the magnetic properties of Ce1−xCuxO2−δ nanorods *Phys. Chem. Chem. Phys.* **17** 3072–80

[16] Maensiri S, Masingboon C, Laokul P, Jareonboon W, Promarak V, Anderson P L and Seraphin S 2007 Egg White Synthesis and Photoluminescence of Platelike Clusters of CeO2 Nanoparticles *Cryst. Growth Des.* **7** 950–5

[17] Wang G, Mu Q, Chen T and Wang Y 2010 Synthesis, characterization and photoluminescence of CeO2 nanoparticles by a facile method at room temperature *J. Alloys Compd.* **493** 202–7